

Chapter 3

Preparation and Investigation of ZnO Nanorods Array Based Resistive and SAW CO Gas Sensors

A. L. Nikolaev, G. Ya. Karapetyan, D. G. Nesvetaev,
N. V. Lyanguzov, V. G. Dneprovski and E. M. Kaidashev

Resistive sensors of carbon monoxide based on zinc oxide nanorod arrays were investigated. ZnO nanorods were produced by pulsed laser deposition (PLD) method at high pressure of argon and carbothermal synthesis. Several constructions of resistive carbon monoxide sensors are obtained. Their resistive properties are investigated. The passive wireless CO sensor on surface acoustic waves (SAW) was studied. The dependence of SAW reflection factor for unidirectional interdigital transducers (IDT) loaded by impedance on its resistance value was investigated. It is shown that the reflection factor varied in linear way versus the value of the resistance in the range from 50 to 400 Ω . The total resistance value for one of the sintered sample lied in the range from 50 to 250 Ω in the case of parallel junction of ZnO nanorods in array by top electrode. This result corresponds to the linear range in the dependence of IDT reflection factor from resistance value. This can be used for determination of small concentrations of CO gas by IDT loaded with impedance based on ZnO nanorod array, because their resistance value depends on CO concentration.

3.1 Introduction

ZnO nanorod arrays are considered as the basic elements for a wide range of new nanoelectronic and nanophotonic devices. In particular, such structures could be used in photodetectors, light emitting diodes, lasers, energy converters, solar cells, electron emitters and chemosensors [1]. Current area of research is the development of wireless CO sensors on surface acoustic waves. As a sensor for CO adsorption, oriented arrays of zinc oxide nanorods currently obtained with laser sputtering [2] or carbothermal synthesis [3] can be used.

A. L. Nikolaev · G. Ya. Karapetyan · D. G. Nesvetaev ·
N. V. Lyanguzov · V. G. Dneprovski · E. M. Kaidashev (✉)
Vorovich Mechanics and Applied Mathematics Research Institute, Southern Federal
University, 200/1, Stachki Ave, Rostov-on-Don, Russia 344090
e-mail: kaidashev@mail.ru

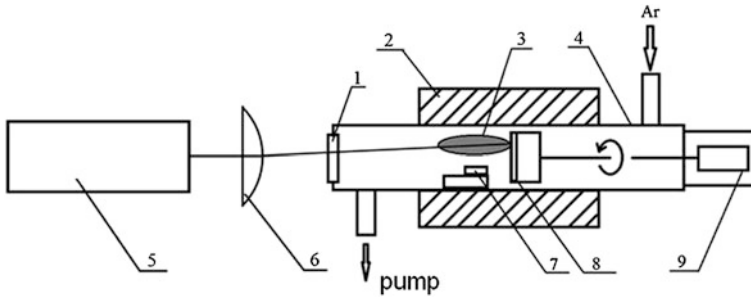


Fig. 3.1 Schematic of the experimental setup for the PLD growth ZnO nanorods

3.2 Experiments and Results

3.2.1 PLD ZnO Nanorods Growth

In our study we investigated the growth of ZnO nanocrystal arrays on sapphire substrates by pulsed laser deposition (PLD) at high pressure of argon [2]. Deposition was carried out in the vacuumized quartz cell with an external resistive heater (Fig. 3.1). Laser radiation of KrF laser ($\lambda = 248$ nm, $E = 300$ mJ) was focused on the surface of rotating ZnO ceramic target. The power density on the target surface was 2 J/cm². Target-substrate distance was 5–35 mm. The repetition frequency of the laser pulses was 3–10 Hz. Synthesis of micro- and nanocrystals was carried out at 12000–24000 laser pulses. The substrate temperature was varied in the range of 850–950 °C. The argon flow was 50 sccm at a pressure of 75–300 mbar. Single crystal substrates of *c*- and *a*-sapphire size $10 \times 10 \times 0.5$ mm³ with buffer layer of ZnO are parallel to the laser plasma plume. To improve the vertical orientation of ZnO nanorods was deposited buffer sub-layer film of zinc oxide. ZnO film was deposited at 10,000 laser pulses, the oxygen pressure was 2×10^{-2} mbar, the substrate-target distance was 70 mm and temperature was 670 °C [4].

Isolated gold nanoparticles were deposited on the surface of the ZnO buffer layer and used as a catalyst for the growth of self-organized ZnO nanorods. Gold nanoparticles (Fig. 3.2) was also obtained by laser deposition in an argon atmosphere ($\lambda = 248$ nm, $Q = 2$ J/cm², $f = 10$ Hz) at $P_{\text{Ar}} = 70$ Pa, $T = 25$ °C, target-substrate distance was $l = 3.5$ cm, the number of laser pulses was $N = 500$). This technique is similar to those reported in [5] and allows one to receive the samples controlling both particle size and number density, virtually without limitations by the nature of the substrate. As seen in Fig. 3.2, gold nanoparticles are isolated from each other and uniformly distributed over the surface of the ZnO buffer layer. The size of Au nanoparticles is about 5–7 nm.

Au nanoparticles were used as a catalyst in PLD of ZnO nanorods under the high pressure of argon [2]. As a result, vertically aligned ZnO nanorods were obtained (see Fig. 3.3). Diameter of nanorods grown via the vapor–liquid–solid process was 60–150 nm, height was 1–2 μ m.

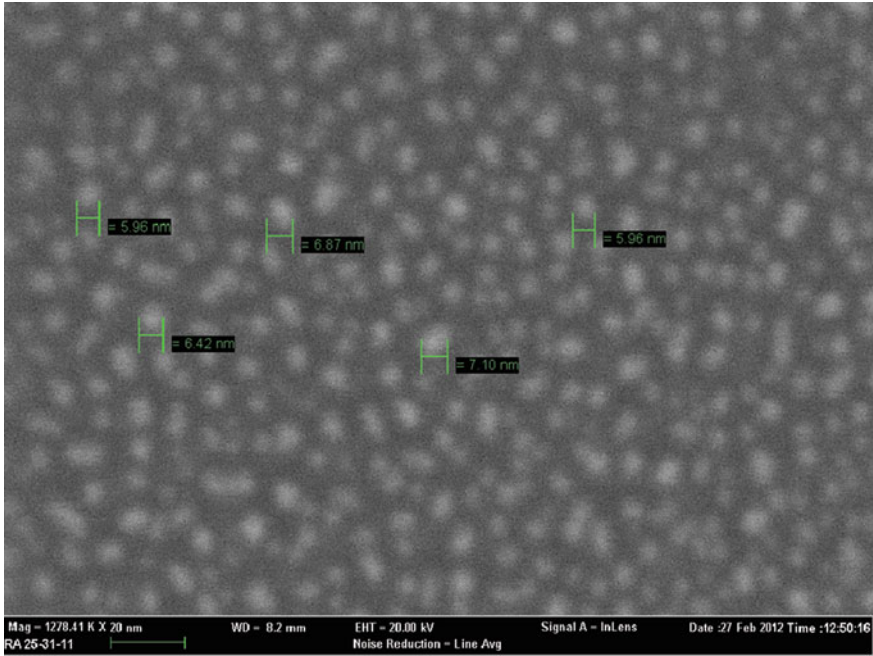


Fig. 3.2 SEM image of gold nanoparticles. Top view of the surface. $P_{Ar} = 70$ Pa, $N = 500$ pulses

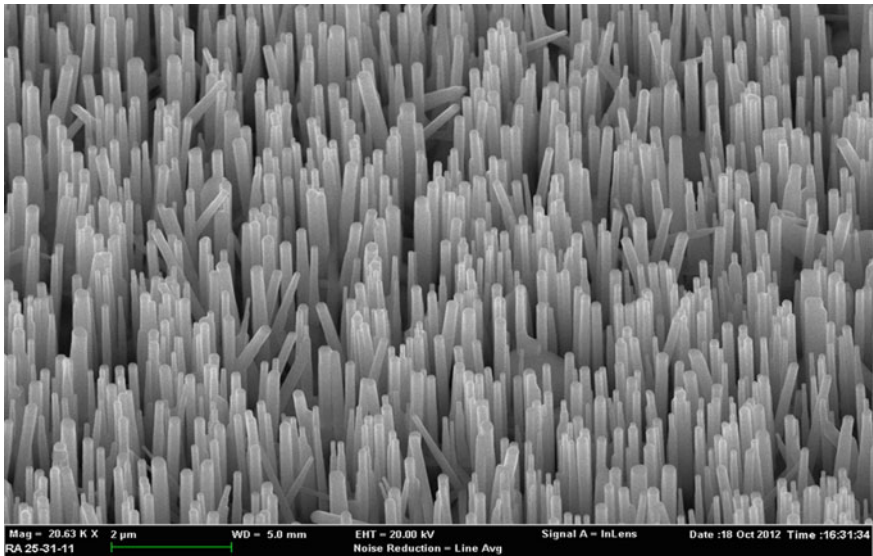
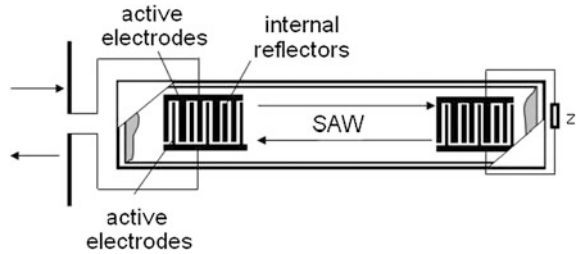


Fig. 3.3 SEM image of ZnO nanorods array, obtained by pulsed laser deposition

Fig. 3.4 Schematic diagram of the wireless SAW CO gas sensor system



3.2.2 Fabrication of the ZnO Nanorods Sensitive Element of SAW Sensor for CO Detection

We have demonstrated the possibility to construct the SAW wireless and passive sensors based on hold-up line comprising two unidirectional IDT for parameter determination of atmosphere [6].

SAW sensor [6] is a delay line (DL) on a surface acoustic wave (SAW) having two unidirectional interdigital transducers (IDT). Firstly, it is connected to the transmitter and receiver antenna, and secondly to reflective IDT–IDT, loaded on the impedance of the sensitive element of the sensor (Fig. 3.4).

Unidirectional IDT produced on substrates (YX/128°-cut lithium niobate) has 17 internal reflectors, and the set of overlapping electrodes with size of 20 lengths of SAW on the frequency of the acoustic matching. IDT on the central frequency of 95 MHz has a width of electrodes equals 10 mm and the set of overlapping electrodes with size of 40 lengths of SAW. As a sensing element for CO we used zinc oxide nanorods array. Reflection coefficient is determined by the frequency dependence of the IDT impedance, followed by Fourier transformation. Figure 3.5 shows the dependence of the reflection coefficient on value of the load resistance. It is seen that this dependence has a minimum of reflection, due to impedance matching of IDT with a 50 Ω load, i.e. most of the energy of SAW is released at the load resistor. This dependence shows that the reflection coefficient for shorted and open unidirectional IDT tends to 1.

The sensing element of SAW sensor consists of a parallel combination of zinc oxide nanorods. Increasing the area of the upper electrode can reduce the total resistance of the associated array of zinc oxide nanorods. The load value Z depends on CO concentration. If you change the resistance of the sensor, then due to the adsorption of CO changes the reflection coefficient of SAW from the reflective IDT. However, as shown in Fig. 3.5, dependence of the reflection coefficient of the unidirectional interdigital transducer on the value of R , connected to an interdigital transducer, is linear load at the site of resistance from 50 to 400 Ω .

Therefore, we developed new design-related arrays of nanorods of zinc oxide having a low total resistance. We have developed a new design of parallel-connected zinc oxide nanorods, the total resistance of which can be varied by changing the area of the upper electrode. The sensors are designed in several phases and the final version of the structure is shown schematically in Fig. 3.6.

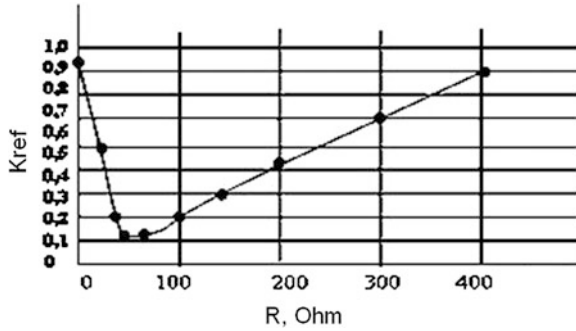


Fig. 3.5 Dependence of reflection coefficient of the unidirectional IDT on load resistance

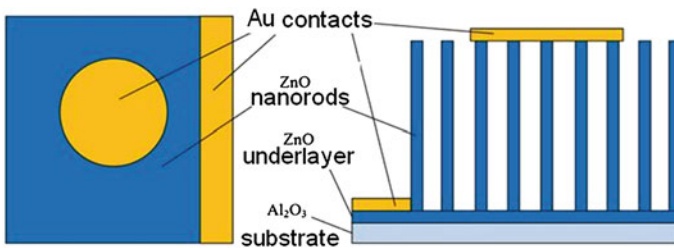


Fig. 3.6 Schematic view of SAW sensing element of CO sensor. Left top view and right side view

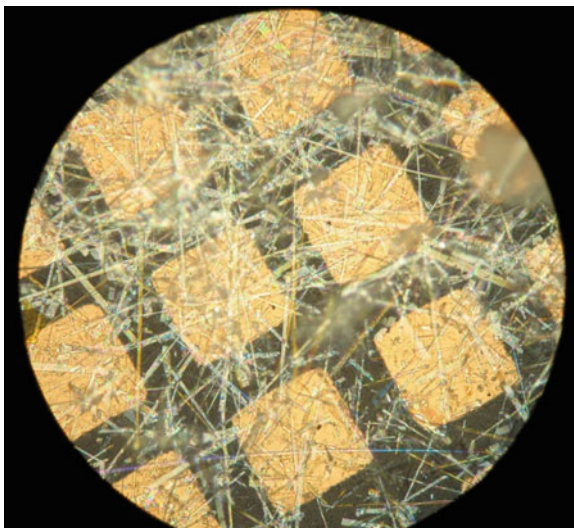
Then the Au electrodes (upper and lower) were deposited by means of PLD for the further investigation of gas-sensing properties of this structure. The lower electrode was deposited on the sample part free from nanorods and the upper one on the top of nanorods. PLD of the upper electrode was carried out at the angle of 45°.

To complete processing the sensor, it was sprayed a nanostructure contact after growth. This sample was placed in a vacuum chamber and lock to the target at the angle of 45° to the target surface. It was also used a masking pattern with a round hole for the deposition of gold contacts on the limited surface area of the sample. Deposition of contact was extended obliquely to gold particles settled on the top of nanorods and not fell to their base. Nanorods screen each other and prevent covering of nanowires base because of its density. Thus, the gold contact is created in the upper part of the nanorods and combines them together.

3.2.3 Resistive CO Sensor Characterization

The sensor design was a series of parallel connected with the nanorods “islands” of Au underlayer. On a quartz substrate was deposited thin-film underlayer by

Fig. 3.7 Sensor's photo obtained by ZEISS Axioskop 40 microscope



pulsed laser deposition through a mask with square holes of the size $a = 90 \mu\text{m}$. The distance between the “islands” was $b = 40 \mu\text{m}$. ZnO nanorods were removed by sonication in a solution of ethanol. The resulting solution of nanorods was applied on the sample surface. Nanorods were annealed in the Au conductive underlayer in Ar atmosphere at $t = 200 \text{ }^\circ\text{C}$ to achieve better electrical contact between rods and sublayer.

The photo given above clearly shows that the individual ZnO nanorods, deposited on the surface of the sample overlap the neighboring gold islands. Thus, as in the case of the above construction sensor of CO, conduction channel from island to island passes through nanorods. Thus, any change in the conductivity of the rods associated with a change in the composition of the surrounding atmosphere, can not affect the total resistance of the sample (Fig. 3.7).

Resistance measurement was carried out using a multimeter Keithley 2000 at constant temperature $t = 250 \text{ }^\circ\text{C}$. CO desorption from the surface of the sample was carried out by blowing measuring chamber with nitrogen gas and continuous UV irradiation of the sample after the measurement. Mutually reversible redox reaction, adsorption–desorption on the semiconductor surface at a constant concentration of CO are in the equilibrium state some time after the lapping CO (Fig. 3.8). By decreasing the concentration of carbon monoxide, the equilibrium shifts toward desorption.

The calculation of the gas sensor's sensitivity occurred by the formula $((R_a - R_b)/R_a) \times 100\%$ where R_a and R_b is the sensor resistance in the presence of CO and in pure air, respectively. Great gas sensor resistance, however, is caused by poor contacts of nanorods with the deposited Au islands. Thus, the sensitivity of the sample was about 250 %. Gas-sensitive properties of the samples are highly dependent on the number of oxygen vacancies [7].

Fig. 3.8 Time dependence of CO sensor sensitivity

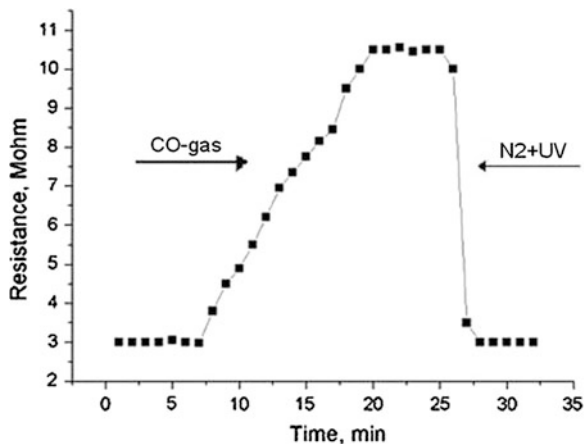
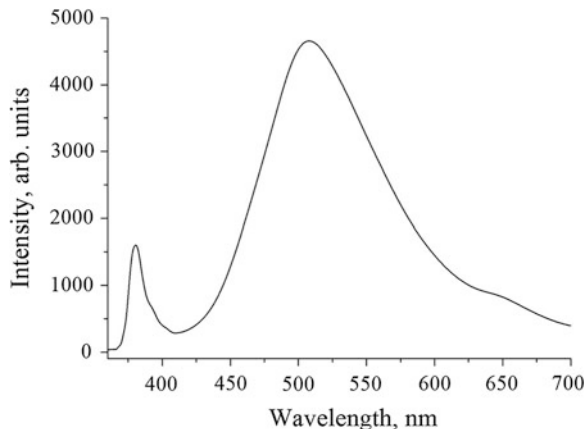


Fig. 3.9 Photoluminescence spectra of the sensor



The ratio of the intensities of the exciton/green regions of the PL spectrum (Fig. 3.9.) was 0.3 for the ZnO nanorods on the surface of the gas-sensitive element. From this ratio, it follows that the concentration of oxygen vacancies in the sample is high. As discussed by authors of the article [7], with increasing the oxygen vacancies sensitivity of the sensor to CO is greatly increased. Chemisorption of O_2^- , O^{2-} and O^- substantially depends on temperature. At low temperatures, mainly occurs O_2^- chemisorption. At a high temperature begins O^- chemisorption, while O_2^- disappears.

3.2.4 SAW CO Sensor Characterization

ZnO nanorods array is the load impedance of one of the ITDs. We have obtained the SAW reflection coefficient dependence on the value of load impedance which

is connected to reflective ITD. This dependence could be used to determine low concentration of gas, for instance, of carbon monoxide. The main goal of our research was fabrication and study of ZnO nanorods sensitive element of SAW sensors for CO detection.

The SAW sensor element sensitive to CO consists of parallel connected ZnO nanorods. In order to decrease the total resistance of ZnO nanorods array we changed the area of upper electrode. The impedance value Z depends on CO concentration. CO absorption influences on the sensitive element resistance resulting in the change of SAW reflection coefficient.

The authors of [7] have studied cathodoluminescence spectra of ZnO nanorods in the visible and ultraviolet regions of the spectrum. Obtained at different temperatures nanorods had a different intensity of the broad band in the green-yellow region of the spectrum of cathodoluminescence associated with oxygen defects in ZnO. By comparing the luminescence intensity in visible and UV region of spectrum, it is possible to make a conclusion about O vacancies in ZnO nanostructures. The photoluminescence spectra (Fig. 3.10) demonstrate the correlation between the sensitivity of samples and the number of O vacancies in nanorods.

By varying nanorods growth temperature from 850 to 915 °C can be produced nanorods with different defectness of oxygen. Because the maximum sensitivity of ZnO at 250 °C [8], the sensitivity measurements were carried out at room temperature and at 250 °C. During heating nanorods to 250 °C from room temperature, the resistance of the connected arrays of ZnO nanorods fell to 6 k Ω . ZnO nanorods array had the load impedance of the reflective ITDs and their total resistance was $R = 6$ k Ω at operational temperature $T = 250$ °C of the sensor. The time dependence of response difference for SAW sensor was obtained. The first response was recorded without CO, the second one—through 8 min after the inflow of gas. These values were normalized with respect to differential response recorded at the end of the first minute after CO inflow (see Fig. 3.11). This dependence indicated that the reflection coefficient had changed. Thus, the ZnO nanostructure obtained could be applied for development of wireless SAW sensors for CO detection.

The low resistance of ZnO nanorods array leads to the maximum value of ITD reflection coefficient. This fact allows us to use this nanostructure as a gas-sensing element of passive noncontact SAW sensor for CO detection. CO was filled with air in the cell capacity of 500 cm³. Gas was fed from the gas cylinder through a regulator with flow rate of 50 cm³/min. The reflection coefficient varied in accordance with the increase of resistance of the nanorods. It happened, apparently, because of the adsorption of carbon monoxide surface of the nanorods. Dependence of the reflection coefficient on the reflective IDT loaded with an array of ZnO nanorods in the first 9 min of the inlet CO recorded by the meter complex transfer «Overview-304/1» with a 1 min interval. To increase the sensitivity of the measurements were taken differential impulse responses. Figure 3.11 shows the difference in response time ($T = 250$ °C without CO and through 8 min after lapping CO) relative normalized difference of response removed after 1 min after lapping CO.

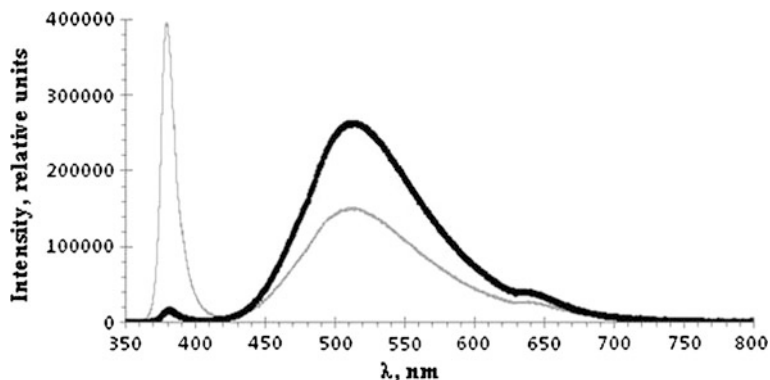


Fig. 3.10 Room-temperature photoluminescence spectra from samples which were grown at different temperatures. Spectrum of the sample grown at 850 °C (*gray line*) and spectrum of the sample grown at 915 °C (*black line*)

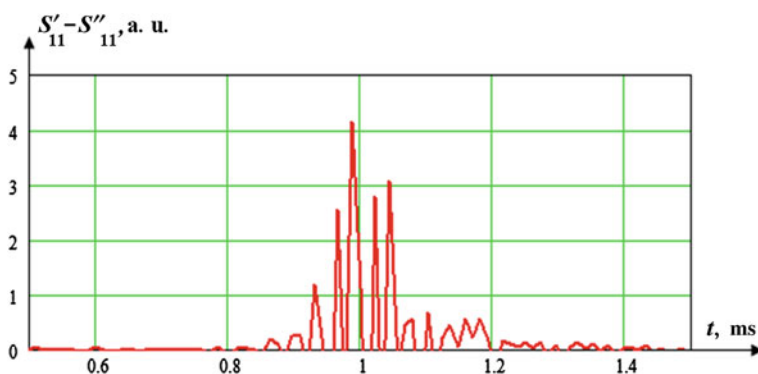


Fig. 3.11 Time dependence of response difference of SAW sensor. The first response was recorded without CO, the second one—through 8 min after the inflow of gas. These values were normalized with respect to differential response recorded at the end of the first minute after CO inflow

If get the resistance values of the nanorods within the maximum sensitivity of the reflection coefficient loaded on IDT resistance [6], it is possible to increase the sensitivity of the sensor to CO. This can be done either by parallel connection of a large number of nanorods, either by increasing the radiation resistance of reflective IDT. However there is a limit, when it is reached the aperture of IDT is decreased. The resistances of a few $\text{k}\Omega$ would be so small that it will lead to significant diffraction of SAW and to inability of correct sensor operation.

However, as shown by the measurements, even when the resistance of the nanorods is $6 \text{ k}\Omega$, change in the difference signal is sufficient to remove the dependence of the reflection coefficient of the resistance change on the nanorods, which is defined as the maximum amplitude of S_{11} parameter.

3.3 Conclusions

ZnO nanorods array with *c*-axis perpendicular to the substrate was grown by pulsed laser deposition at high pressure of argon and carbothermal synthesis. It was fabricated and tested sensing element of SAW sensor of CO being an array of parallel connected zinc oxide nanorods. It is proposed to use the photoluminescence method for the optimization of ZnO nanorods growth with maximum sensitivity to CO. We used this method to find synthesis temperature at which the sensitivity of the device is the highest.

Acknowledgments This work has been supported by the Ministry of Education and Science of Russian Federation, project No 2.5896 “The development of methods to obtain and study the properties of semiconductor nanostructures to create the elements of nanophotonic devices”, and by the internal funding of the Southern Federal University “The research and development of technological bases to produce the nanostructured ZnO and VO_x films for application as sensitive elements of sensors” (Nano-011, SFedU).

References

1. S.K. Youn, N. Ramgir, C. Wang, K. Subannajui, V. Cimalla, M. Zacharias, *J. Phys. Chem. C* **114**, 10092 (2010)
2. M. Lorenz, E.M. Kaidashev, A. Rahm, Th Nobis, J. Lenzner, J.G. Wagner, D. Spemann, H. Hochmuth, M. Grundmann, *Appl. Phys. Lett.* **86**, 143113 (2005)
3. N.V. Lyanguzov, V.E. Kaydashev, E.M. Kaidashev, K.G. Abdulvakhidov, *Tech. Phys. Lett.* **37**(3), 193 (2011)
4. E.M. Kaidashev, M. Lorenz, H. Wenckstern, G. Benndorf, A. Rahm, H.-C. Semmelhack, K.-H. Han, H. Hochmuth, C. Bundesmann, V. Riede, M. Grundmann, *Appl. Phys. Lett.* **82**(22), 3901 (2003)
5. C.D. Andrea, F. Neri, P.M. Ossi, N. Santoand, *Nanotechnology* **20**, 245606 (2009)
6. G.Y. Karapetyan, V.G. Dneprovski, A.S. Bagdasaryan, S.A. Bagdasaryan, A.L. Nikolaev, E.M. Kaidashev, *Ingenery Vestnik Dona* **2**, (2012) (in Russian)
7. T.-J. Hsueh, Y.-W. Chen, S.-J. Chang, S.-F. Wang, C.-L. Hsu, Y.-R. Lin, T.-S. Lin, I.-C. Chene, *J Electrochem Soc* **154**(12), 393 (2007)
8. J.X. Wang, X.W. Sun, H. Huang, Y.C. Lee, O.K. Tan, M.B. Yu, G.Q. Lo, D.L. Kwong, *Appl. Phys. A* **88**, 611 (2007)